



Investigation of Optimum Structures at Submarine Pressure Hulls under Hydrostatic Pressure with Finite Element Method

 Burak Eyiler¹,  Ertekin Bayraktarkatal²

¹Department of Naval Architecture and Marine Engineering, National Defense University, Turkish Naval Academy, İstanbul, Türkiye

²Department of Naval Architecture and Marine Engineering, İstanbul Technical University, İstanbul, Türkiye

To cite this article: B. Eyiler, and E. Bayraktarkatal. Investigation of optimum structures at submarine pressure hulls under hydrostatic pressure with finite element method. *J Nav Architect Mar Technol.* 2024;226(2):25-35.

Received: 16.05.2024 - **Revised:** 12.11.2024 - **Accepted:** 12.11.2024 - **Publication Date:** 31.01.2025

Abstract

In this study, the optimum structure of submarine pressure hulls under hydrostatic pressure was investigated by finite element method. The weight/volume ratio, which is considered as the buoyancy factor, and the maximum strength were taken as the basis for structural efficiency in the submarine pressure hull design. The collapse diving depth pressure was used for both the scantling of structural components and the calculation of critical buckling pressures. General instability buckling shape was observed during the analysis and the results were verified by DNV-GL Classification Society rules. Finally, the results of the different structures optimized to give the maximum strength at the same weight were presented in tables.

Keywords: Ultimate strength, finite element method, cylindrical shells, buckling, general instability

1. Introduction

The structural stability of submarines is very important for them to carry out their missions without any problems. Accidents at submarines from the past to the present have made these studies valuable for both the safety of the crews and the survival of the structure. Finally, the accident on the Titan submarine, which was planned to dive to a depth of 3800 meters to see the wreckage of the Titanic and resulted in the death of five people, showed the importance of these studies [1].

Submarines generally have two hulls. The first of these hulls is the pressure hull, which contains the living spaces, weapon

control systems, weapons communication and control room, batteries, main and auxiliary machinery and provides the strength of the submarine under hydrostatic pressure. The function of the outer shell covering the submarine pressure hull is to add a hydrodynamic feature to the structure [2,3].

Experimental and numerical studies on the strength of cylindrical shells have been studied in the past. The first theoretical solutions for cylindrical shells of uniform thickness were presented by Von Mises, Windenburg and Trilling and Von Sanden and Gunther in 1929, 1934 and 1952 respectively. These theories are still used because they are relatively simple [4].

Address for Correspondence: Burak Eyiler, Department of Naval Architecture and Marine Engineering, National Defense University, Turkish Naval Academy, İstanbul, Türkiye

E-mail: burak.eyiler@gmail.com

ORCID ID: orcid.org/0000-0003-1723-7605

For the calculation of symmetric buckling of a cylindrical shell between stiffeners, Lunchick [5] presented the report numbered 1393 called “plastic axial symmetric buckling of stiffened cylindrical shell made of strain hardening materials and subjected to external hydrostatic pressure”. In this study, Lunchick [5] took the hardening behaviour of the material into the calculation and considered the Poisson ratio as a variable ranging from its elastic value to $1/2$, which is the upper limit for an incompressible material. He presented a shell length criterion for long and short cylinders. He said that below this value the shell buckles in only one half-wave [5].

For the asymmetrical buckling calculations of the stiffened cylindrical shell, Reynolds [6] presented the report numbered 1392, named inelastic buckling of the cylindrical shell under hydrostatic pressure. In this report, a solution of Gerard’s differential equations for plastic buckling of cylindrical shells was found by Reynolds [6] for asymmetric buckling under hydrostatic pressure. According to this study, the critical buckling pressure was found as a function of the cylindrical shell geometry and the secant and tangent moduli for the shell material according to the stress-strain diagrams [6].

For the calculation of the general instability buckling shape of stiffened cylindrical shells, Bryant [7] presented his report number 306, named buckling of a stiffened cylindrical shell under hydrostatic pressure. In his paper, Bryant [7] solved the general instability problem by using the elastic potential energies of the shell and girders.

Aileni et al. [8] calculated the critical buckling pressure of stiffened cylindrical shells under external pressure using finite element method (FEM). Linear and nonlinear buckling analysis results were compared with experimental results and it was observed that the nonlinear analysis results were closer to the experimental results. The variation of critical buckling pressures was investigated by using reinforcing elements in Z, square, rectangular, C, I and T sections. At the end of the analysis, it was observed that the critical buckling pressure decreased as the distance between the reinforcements increased. In addition, it was found that higher critical buckling pressures occurred in Z and square section reinforcements [8].

Oh and Koo [9] analysed 7 case studies with analytical solutions for the optimum design of submarine pressure hull and validated the study with finite element analysis. As a result of the study, they proposed initial scantling formulas for weight optimization in relation to radius (R), yield strength and design pressure for shell thickness, flange width, flange thickness, web height and web thickness. Using the proposed initial sizing formulas, it was found that the pressure hull weight was reduced between 6% and 19% [9].

Kine [10] aimed to optimize the buckling performance of a pressure hull under hydrostatic pressure. His study was based on the critical buckling pressure and the weight corresponding to this pressure. The optimization includes four design parameters including cylindrical shell thickness, unsupported length between stiffeners, stiffener height and stiffener thickness. The results obtained from this study indicated that the critical buckling pressure increased by 7.09%. It was found that the unsupported length between reinforcements and cylinder thickness have a significant effect on the buckling performance of the pressure hull [10].

Wei et al. [11] investigated the optimization of a trapezoidal reinforced composite cylindrical pressure hull under hydrostatic pressure. The composite cylindrical shell was manufactured with carbon fiber reinforced epoxy, while the stiffeners were made of aluminium alloy. An analytical buckling model was derived for the stiffened composite cylindrical shell under hydrostatic pressure. Then, the FEM was used to verify the accuracy of the analytical solution. After verification, the analytical solution was combined with the genetic algorithm to obtain the maximum buckling pressure and optimize the cross-sectional shape of the stiffeners. It was found that there is a linear relationship between the cross-sectional moments of inertia of the stiffeners and the critical buckling pressure [11].

Rathinam et al. [12] generated finite element models with the help of the Ansys package to predict the shell and general instability damage shapes in stiffened cylindrical shells. Finite element analysis results were compared with analytical and experimental results. As a result, it was found that the minimum critical pressure value determines in which buckling mode the pressure hull will be damaged [12].

Şenol [13] presented a structural optimization based on the FEM for the optimum structural design of a submarine pressure hull. He compared the finite element results with the DNV-GL Classification Society results and observed that they converged. In his studies to determine the optimum geometry, a single ring stiffened geometry with effective shell length was subjected to external hydrostatic pressure using non-linear material properties and large deformations. As a result, an optimum design is defined in a way to obtain the minimum weight and maximum internal volume targets [13].

Fu et al. [14] proposed a pressure hull design method within the limits of outer envelope size and inner space utilization using variable section ribs. The pressure hull bearing mechanism was theoretically and numerically calculated and experimentally verified. They used the energy method to calculate the critical buckling pressure. As a result, it was found that variable cross-section ribs increase the buckling load by about 26.7% by maximizing the space utilization [14].

Shinoka and Netto [15] conducted three different optimization studies to minimize the weight of submarine pressure hulls. The optimization tools used were: Differential Evolution, Particle Swarm and Simulated Annealing. As a result, they found that the Differential Evolution algorithm is the most reliable and consistent in minimizing the objective functions [15].

In this study, the optimum structure was investigated for submarine pressure hulls where different reinforcements are used. The FEM was used to calculate the critical buckling pressure and the Screening optimization method was used to calculate the optimum structure. The results of the analysis were also verified with DNV classification society rules. When these results were analyzed in terms of structural efficiency, it was determined that the structures with Transverse Internal Reinforced Systems were the most effective.

2. Submarine Pressure Hull Design

2.1. Calculation of Safety Factor and Diving Depth Pressures

The pressure hull is the basic structure of a submarine and it constitutes half or more of the total weight of the submarine. A typical pressure hull is produced by welding T-section girders to high-strength axisymmetric shells produced by cold rolling. Since the late 1970s, the typical form of a submarine pressure hull has been a ring stiffened circular cylindrical shell, closed by a parabolic bow and an elliptical stern hatch, as shown in Figure 1 [16,17].

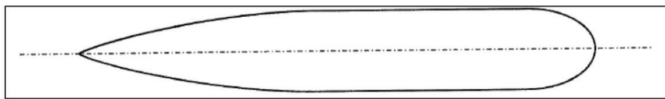


Figure 1. Submarine hull form [18].

The biggest problems faced by the submarine designer are to reduce the weight of the pressure hull and the cost of submarine construction, to increase the payload carrying capacity and the ship's speed.

There are some diving depths that form the basis for submarine pressure hull design. These depths are mainly: Nominal diving depth (NDD) is the diving depth at which the submarine can operate unrestrictedly. Collapse diving depth (CDD) is the theoretical maximum depth at which the submarine can dive. Collapse diving pressure (CDP) is the pressure value at which the pressurized hull can collapse under a 1-minute load. This depth value is used for the scantling of pressure hull structural components [19,20].

The conventional submarine considered in this study was assumed to operate at a NDD of 400 meters. The DNV-GL

Classification Society gives the calculation of the hydrostatic pressure depending on the NDD in Equation 1 as follows [19].

$$\text{Nominal Diving Pressure} = \text{Nominal Diving Depth} \cdot 0.101 \text{ (bar)} \quad (1)$$

According to the calculation, it was found that the submarine would be exposed to 40.4 bar a hydrostatic pressure at the NDD, which would be 4.04 MPa because 1 bar pressure corresponds to 0.1 MPa pressure.

Considering the constraints given in Table 1, the safety factors S_1 and S_2 corresponding to the nominal diving pressure of 40.4 bar were found to be 1.20 and 1.7984 respectively. The CDP was found 7.26554 MPa and the Test diving pressure applied to test the tightness and function of the pressure hull and equipment was found 4,848 MPa.

Table 1. Determination of safety factors for test and collapse diving pressure in relation to nominal diving pressure [19].

Nominal diving pressure (bar)	10	20	30	40	50	≥60
$S_1 = \text{TDP/NDP}$ (2)	1.40	1.25	1.20	1.20	1.20	1.20
$S_2 = \text{CDP/NDP}$ (3)	2.40	2.00	1.87	1.80	1.76	1.73

1. Minimum nominal diving pressure 5 bar
 2. In the range NDP = 5 30 bar: $S_1 = 3/\text{NDP} + 1.1$
 3. In the range NDP = 5 60 bar: $S_2 = 8/\text{NDP} + 1.6$
 4. If Depth > Nominal Diving Depth, the minimum value of S_2 is 2.

2.2. Structure Material

Pressure hull materials must be able to withstand high external pressures and the adverse effects of the environment. The commonly used material for a submarine pressure hull is steel with high yield strength, usually obtained by alloying or heat treatment. HY grade steels are metallurgically quenched and tempered martensitic steels. This martensitic lattice structure is formed as a result of heat treatment with alloying elements such as nickel, chromium, molybdenum and vanadium. Table 2 shows the general physical properties of the materials used in the construction of submarine pressure hulls. In this study, HY100 steel was preferred [21,22].

Table 2. Material properties of HY80, HY100 and HY130 [9].

Property	HY80	HY100	HY130
Young's modulus (E)(GPa)	206	206	206
Poisson's ratio (ν)	0.3	0.3	0.3
Density (ρ , kg/m ³)	7746	7850	7885
Yield Strength ($\sigma_{0.2}$, MPa)	552	686	890
Maximum tensile strength (σ_u , MPa)	611	760	986
Elongation (%)	19	17	14

2.3. Scantling of Structural Components

The strength and stiffness of any structure vary according to the properties of the material used and the geometry of the structure. Without changing the geometry of a structure, the strength and stiffness of the structure can be increased by adding small weight stiffeners to the structure. It has been observed that the buckling strength of the hull is greatly improved by using stiffeners. In pressure hulls, T-section stiffeners are most commonly used and are usually placed inside the hull. In this study, different stiffeners with the same cross-sectional moment of inertia were used for transverse, longitudinal and both transverse and longitudinal (combined) systems [8]. Figure 2 shows the effective length shell with T-section stiffeners.

Oh and Koo [9] proposed initial sizing formulas for shell thickness, flange width, flange thickness, web height and web thickness based on R, yield strength and design pressure in their study on the optimum design of submarine pressure hull. These formulas are given in Table 3. In this study, these formulas were used for the initial sizing.

In this study, the R was defined as 3123 mm, and the length of the pressure hull was specified as 9369 mm.

The structure lengths obtained depending on the input parameters were given in Table 4.

For the scantling of the frame space, the effective length formula in Equation 2 in the fourth chapter of the DNV-GL Classification Society Rulebook was used [19].

$$L_{eff} = \frac{2}{\sqrt[4]{3(1-\nu^2)}} \sqrt{R_m \cdot s} \quad (2)$$

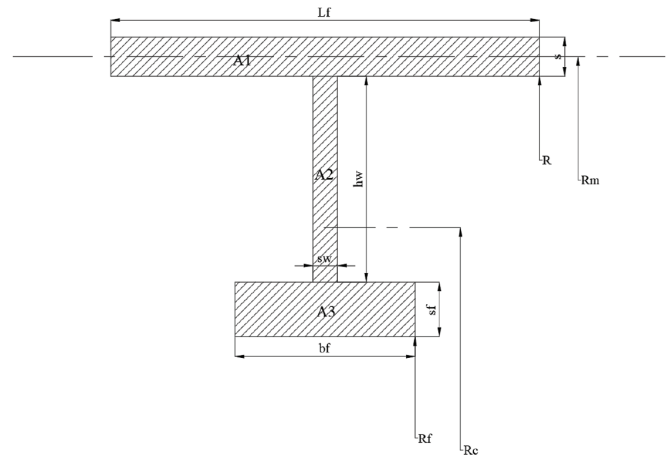


Figure 2. Pressure hull frame geometry [19].

Table 3. Empirical formulas proposed by Oh and Koo [9].

Shell Thickness (h) (mm)	Frame Space (Lfr) (mm)	Web Height (hw) (mm)	
$h = 0.790 \frac{pR}{\sigma_{0.2}}$	$L_{fr} = 1,557 \sqrt{Rh}$	$h_w = 7,552h$	$h_w = 5,966 \frac{pR}{\sigma_{0.2}}$
Web Thickness (sw) (mm)			
$s_w = 0.645h$	$s_w = 0.0866 h_w$	$s_w = 0.510 \frac{pR}{\sigma_{0.2}}$	-
Flange Width (bfl) (mm)			
$b_{fl} = 3,827h$	$b_{fl} = 0.507 h_w$	$b_{fl} = 3,025 \frac{pR}{\sigma_{0.2}}$	-
Flange Thickness (tfl) (mm)			
$t_{fl} = 1,414h$	$t_{fl} = 0.369 b_{fl}$	$t_{fl} = 1.12 \frac{pR}{\sigma_{0.2}}$	-

Table 4. Structural lengths.

Shell Thickness (h) (mm)	Frame Space (Lfr) (mm)	Web Height (hw) (mm)	
$h = 26.13$	$L_{fr} = 444.90$	$h_w = 197.39$	$h_w = 197.38$
Web Thickness (sw) (mm)			
$s_w = 16.85$	$s_w = 17.09$	$s_w = 16.87$	-
Flange Width (bfl) (mm)			
$b_{fl} = 100.02$	$b_{fl} = 100.077$	$b_{fl} = 100.08$	-
Flange Thickness (tfl) (mm)			
$t_{fl} = 36.95$	$t_{fl} = 36.91$	$t_{fl} = 37.05$	-

The structural component lengths chosen as a result of the scantling were given in Table 5.

Table 5. Structural component lengths of the pressure hull.	
Pressure hull length	9,369*
Shell thickness (s)	27
Web height (h _w)	197
Web thickness (s _w)	17
Flange width (b _f)	100
Flange thickness (s _f)	37
Frame space (L _f)	453
*All units in mm.	

The moment of inertia of the singular ring stiffener with reference to the neutral axis was calculated as 7.70536.108 mm⁴ (Parallel Axis Theorem).

3. Calculation of Critical Buckling Pressure of Submarine Pressure Hull

When a submarine pressure hull is exposed to a pressure equal to or exceeding the CDD during operation, the hull may experience the following types of damage:

1. Asymmetric Interstiffener Buckling
2. Symmetric Interstiffener Buckling
3. General Instability
4. Tripping of Frames
5. Fore and Aft Buckling [23].

Some of the factors affecting the buckling shape of ring stiffened cylindrical shells are the bending stiffness of the frames and the cylindrical shell, the type of stiffeners such as longitudinal, ring or combination of these two [10].

Buckling shapes for stiffened cylindrical shells can be classified into two main groups. These are interstiffener (local) buckling and general instability of the structure. In local buckling, if the bending stiffness of the frames is such that they will not buckle when subjected to a critical load, the shell will buckle between the frames. This buckling is classified as asymmetric and symmetric interstiffener buckling [10].

Asymmetric buckling is also called lobe buckling and occurs when the sizes of the frames are small and they are located far apart from each other. As shown in Figure 3, the shell buckles in a wave along the circumference between the frames [18].

Symmetrical buckling occurs when the ring stiffeners have large dimensions and are placed very close to each other. As shown in Figure 4, the cylindrical shell buckles in the shape of an accordion [18].

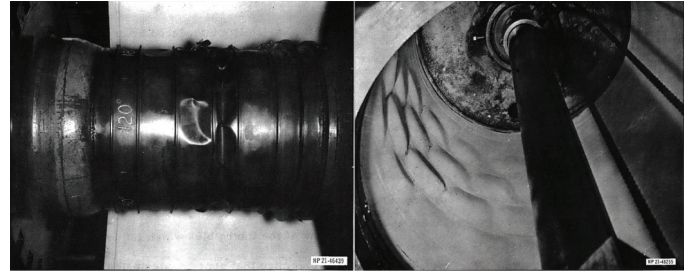


Figure 3. Asymmetric buckling failure [24].

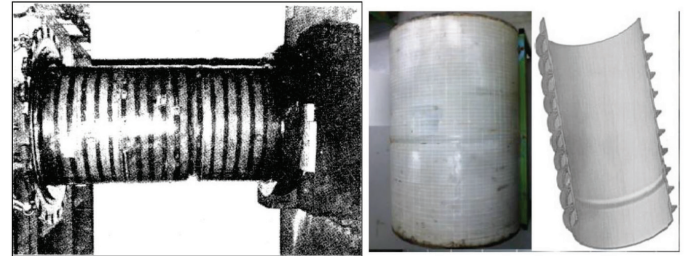


Figure 4. Symmetrical buckling failure [18].

General instability of the structure is described as buckling of the pressure hull between bulkheads, web frames or dished ends. In this buckling mode in order to resist displacements in the shell, there isn't enough bending stiffness in the frames [18].

In our design, general instability buckling mode was found in our finite element analysis. This failure mode is caused by a lack of strength of the material or the submarine diving deeper than the collapse depth [18]. Figure 5 shows the general instability buckling shape.

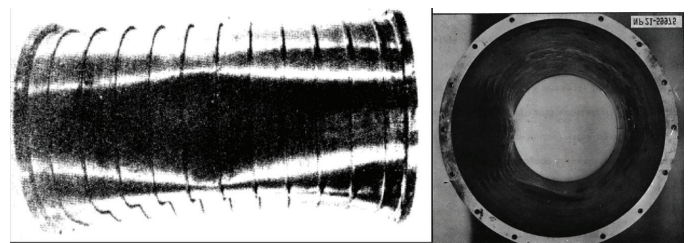


Figure 5. General instability buckling failure [18,24].

DNV-GL Classification Society equations for the calculation of the general instability critical buckling pressure are as follows [19]:

The membrane pressure:

$$P_m = \frac{E \cdot s}{R_m} \cos^3 \alpha \frac{\beta^4}{(n^2 - 1 + \beta^2/2)(n^2 + \beta^2)^2} \quad (3)$$

The pressure in the web frames:

$$P_D = \frac{2 \cdot (n^2 - 1) \cdot E \cdot I_D \cdot \cos^3 \alpha}{R_{c,D}^2 [R_m - 4(R_m - R_{c,D})] (L_D + L_{D,lr})} \cdot \frac{n^2 - 1}{n^2 - 1 + \beta_B^2 / 2} \quad (4)$$

The pressure in the frames:

$$P_F = \frac{(n^2 - 1) \cdot E \cdot I_F \cdot \cos^4 \alpha}{R_{c,F}^3 \cdot L_F} \cdot \frac{n^2 - 1}{n^2 - 1 + \beta^2 \frac{1}{2} \frac{P_D}{P_D + P_m}} \quad (5)$$

The pressure in the bulkheads:

$$P_B = \frac{E \cdot s}{R_m} \cos^3 \alpha \frac{\beta_B^4}{(n^2 - 1 + \beta_B^2 / 2) (n^2 + \beta_B^2)^2} \quad (6)$$

The general instability pressure:

$$P_g^n = P_F + \frac{P_m \cdot P_D}{P_m + P_D} + P_B \quad (7)$$

Table 6 shows the general instability critical buckling pressure and its components.

Table 6. General instability critical buckling pressure results.	
Pressures (MPa)	
The membrane pressure:	2.483
The pressure in the frames:	23.8474
The pressure in the bulkheads:	2.483
The pressure in the web frames:	0
General instability pressure:	26.3312

4. Finite Element Analysis and Optimization Method

In this part of the study, the finite element analyses were used to validate the critical buckling pressures found in the previous section and to optimize the structure.

The criteria defined for the optimum design:

$$CDP \leq P_{cr_asym}$$

$$CDP \leq P_{cr_sym}$$

$$CDP \leq P_g$$

Minimum Buoyancy Factor

Eigenvalue buckling analysis is used to determine the theoretical critical buckling load of an ideal linear elastic structure. It is assumed that the initial imperfections of the structure are neglected. It is used to predict the bifurcation point using a linearized model of an elastic structure. A full 360 degree model is required for the analysis. Because buckling occurs, the deformation of the structure is no longer axisymmetric [10].

To determine the buckling load factor λ for the structure under pressure P, a linear static analysis is first performed. In the eigenvalue problem given in Equation 8, K is the stiffness and S is the stress matrix of the structure. These are calculated by static analysis with prestressing effects established. The solution of the eigenvalue problem gives the i. eigenvalue λ_i (buckling load factor), where ψ_i is the i. eigenvector of the displacement corresponding to the eigenvalue. Not all eigenvalues are necessary and the critical buckling load is calculated with the lowest eigenvalue [25].

$$(K + \lambda_i S) \Psi_i = 0 \quad (8)$$

Depending on the buckling load multiplier obtained at the end of the linear buckling analysis, the critical buckling pressure is calculated as given in Equation 9 [26].

$$\text{Buckling Load Factor} = \frac{\text{Critical Buckling Pressure}}{\text{Applied Load}} \quad (9)$$

The critical load multiplier was calculated here:

If $\lambda_c < 1$, the structure buckles.

If $\lambda_c > 1$, the structure is safe.

4.1. The Geometry Design

The structure was designed as a shell element. Within the scope of the design, 21 frames with a distance of 453 mm between them were used. Figure 6 shows the design process of the structure.

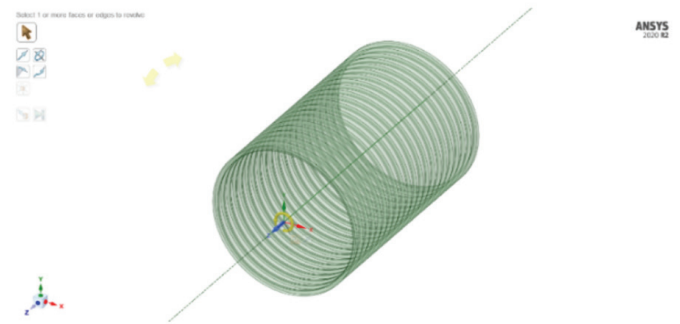


Figure 6. Pressure hull design.

4.2. Mesh Generation

When the convergence analysis was examined in Table 7, the result obtained using a mesh element size of 30 mm was taken as the reference value. According to this value, the deviation amounts from this value for other element sizes were given as percentages. When the average mesh quality, minimum mesh quality and percentage change

Table 7. Mesh convergence analysis.

Element size	Buckling load factor	Critical buckling pressure	Minimum mesh quality	Average mesh quality	% Change
30	3.49725	25.40941	0.988799	0.995736	Reference result
40	3.49901	25.4222	0.911797	0.971807	0.050339
50	3.50288	25.45032	0.948748	0.989762	0.161003
60	3.504644	25.46313	0.982792	0.991556	0.211425
70	3.506927	25.47972	0.925332	0.971309	0.27671
80	3.509487	25.49832	0.911796	0.972581	0.349917
90	3.513275	25.52584	0.862857	0.965442	0.458238
100	3.514704	25.53622	0.781301	0.917871	0.499084

values generated depending on the mesh element size were examined, it was seen that the most ideal mesh size was 50 mm. Analyses were continued using a mesh size of 50 mm.

The cross-sectional view of the structure as a result of the meshing process was shown in Figure 7.

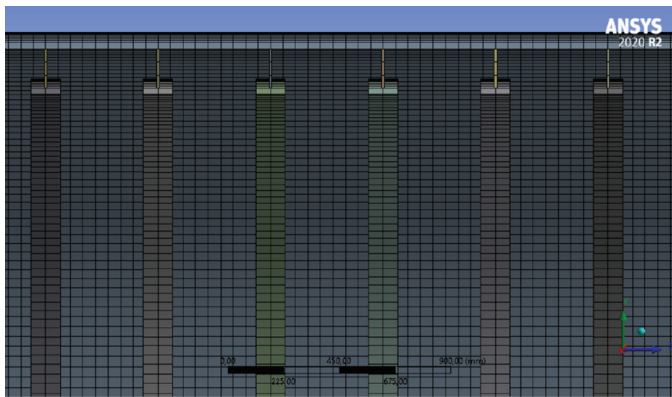


Figure 7. Cross-sectional view of pressure hull.

4.3. Load and Boundary Conditions

The linear buckling analysis of our pressure hull model was analyzed under a collapse buckling pressure of 7.26554 MPa. It was accepted that the pressure hull was constrained by bulkheads and the two ends of the hull are supported by fixed supports.

4.4. Buckling Analysis

After the mesh model of the pressure hull model was designed and the load and boundary conditions were entered into the system, the static analysis was performed first. Following this static analysis, the results obtained were linked to the buckling analysis and the first linear buckling analysis of the structure was done. Figure 8 shows the buckling mode of the structure as a result of buckling analysis.

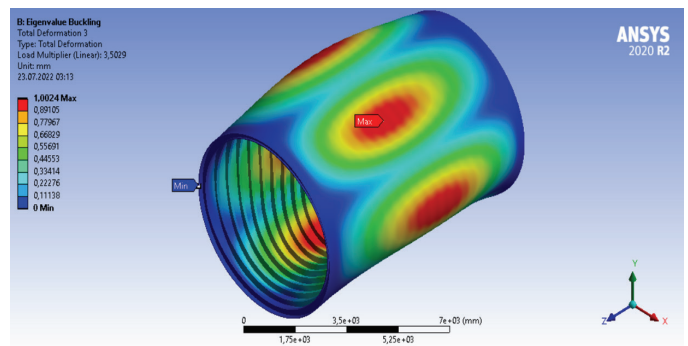


Figure 8. First linear buckling analysis.

5. Investigation of the Optimum Submarine Pressure Hull

In this section, the Screening optimization method was used to determine the ideal design in the model analyzed and to realize the objective functions mentioned in the previous sections. Within the scope of the optimization study, shell, web and flange thicknesses were considered as input parameters, while the pressure hull weight, internal volume and buckling load factor were considered as output parameters. Depending on the changing input parameters in the cylindrical pressure hull geometry, it was desired to resize the structure and recalculate the buckling calculations.

The Screening method can be used for both Response Surface Optimization and Direct Optimization systems. This method enables you to create a new set of samples and order the samples according to the objectives and constraints. This non-iterative method can be used for any type of input parameter. Screening is typically used to find initial candidate points for preliminary design. These candidate points can subsequently serve as initial points for gradient-based methods to refine the solution. Three candidate designs were selected from 9000 samples. The shell, web and flange thicknesses used

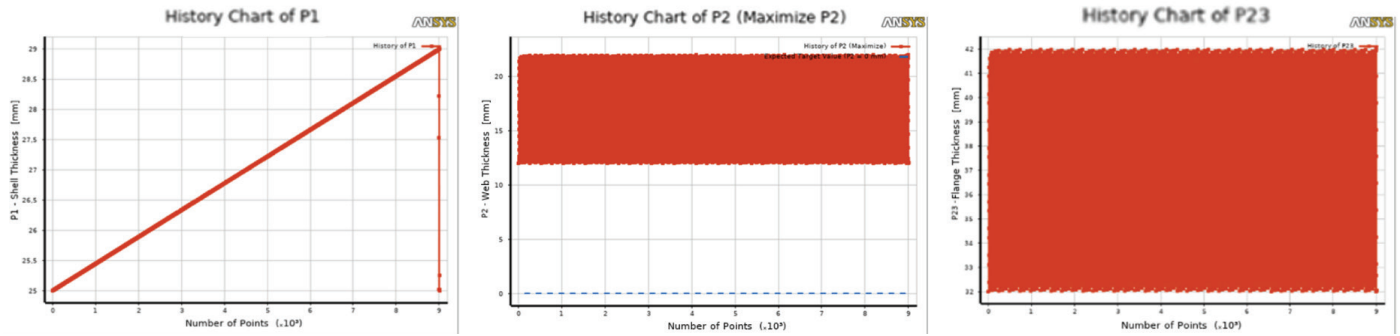


Figure 9. Shell, Web and Flange thickness sample diagram.

in the design scheme created for the optimization study are shown as graphs in Figure 9, respectively [26].

The 9000 sample design points generated within the scope of the optimization and the related output parameters are shown in Figure 10. Here, the points shown in gray are the samples that are out of the targets.

The influence of the input parameters on the output parameters is shown in Figure 11. As can be seen from the graph, the flange thickness has a high sensitivity with the buckling load factor and a much lower sensitivity with the mass of the structure compared to the shell and web thickness.

From the 9000 samples analyzed, 3 design points were identified by Ansys. These 3 candidate design points are shown in Figure 12.

A comparison of the optimized geometry and the initial geometry is given in Table 8.

5.1. Designs Using T-Section Stiffeners

Different designs using T-section stiffeners in the optimization stage are shown in Figures 13, 14, 15, and 16, respectively.

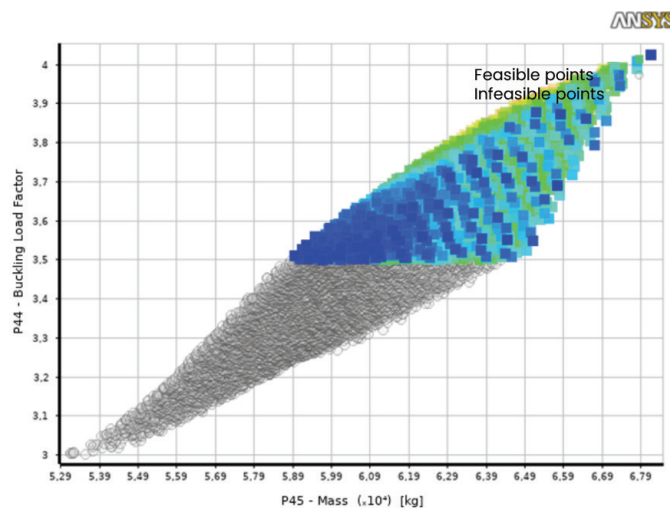


Figure 10. Design points and corresponding output parameters.

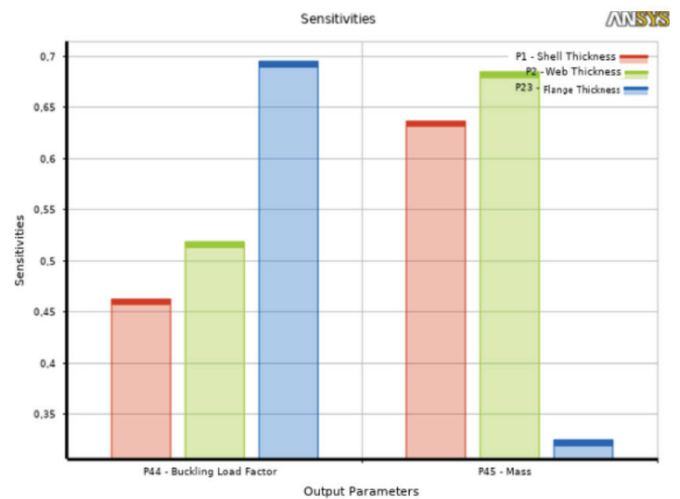


Figure 11. Sensitivity of parameters.

Candidate Points			
	Candidate Point 1	Candidate Point 2	Candidate Point 3
P1 - Shell Thickness (mm)	25,092	25,716	26,332
P2 - Web Thickness (mm)	✗✗ 16,493	✗✗ 15,218	✗✗ 13,79
P23 - Flange Thickness (mm)	41,466	41,557	41,883
P44 - Buckling Load Factor	★★ 3,5121	★★ 3,5034	★★ 3,5029
P45 - Mass (kg)	✗✗ 58957	✗✗ 59099	✗✗ 59205

Figure 12. Candidate design points identified by the optimization tool.

Table 8. Comparison of initial buckling analysis and optimized analysis.		
Support element	T profile	T profile
Flange thickness	37	41.5
Web thickness	17	16.5
Shell thickness	27	25
Buckling load factor	3.502	3,512
Critical buckling pressure	25.450	25.517
Structure mass (kg)	60670.43	58956.89
Internal volume (m ³)	245.66	244.90

The optimization results for the T-sections stiffened systems are given in Table 9.

5.2. Designs Using Flat Bar Stiffeners

Different from the T-sections stiffened systems, the change of buckling behavior was investigated by using flat bar stiffeners in the structure. The flat bar stiffeners to be used

should have an equal moment of inertia with the T-section reinforcing element. The flat bar reinforced systems with different layouts are shown in Figures 17, 18 and 19, respectively.

The optimization results for the flat bars stiffened combined system are given in Table 10.

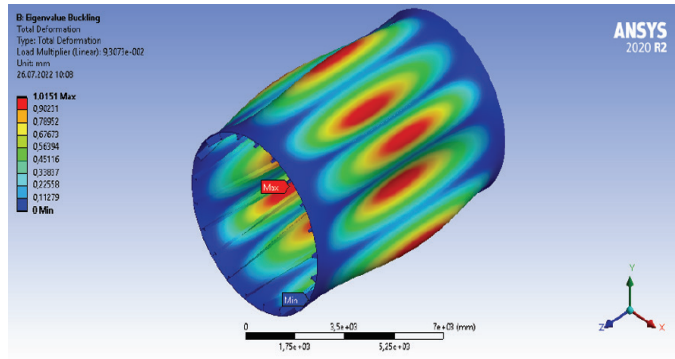


Figure 13. Twenty one T-sections stiffened longitudinal system isometric view.

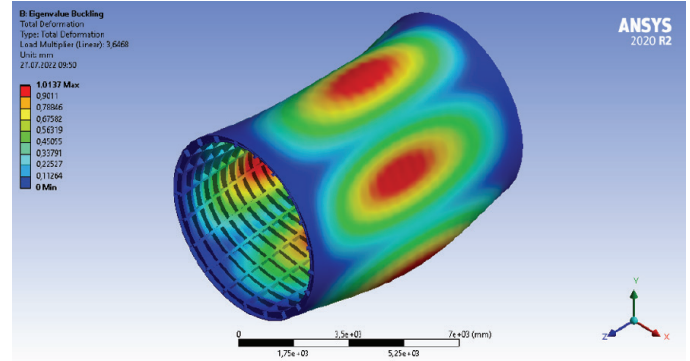


Figure 15. T-sections stiffened combined internally system isometric view.

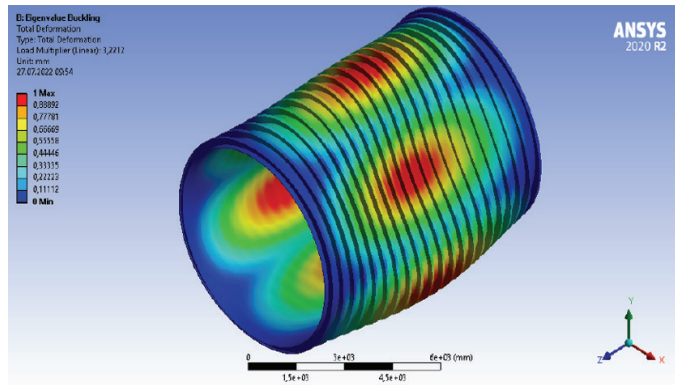


Figure 14. T-sections stiffened externally system isometric view.

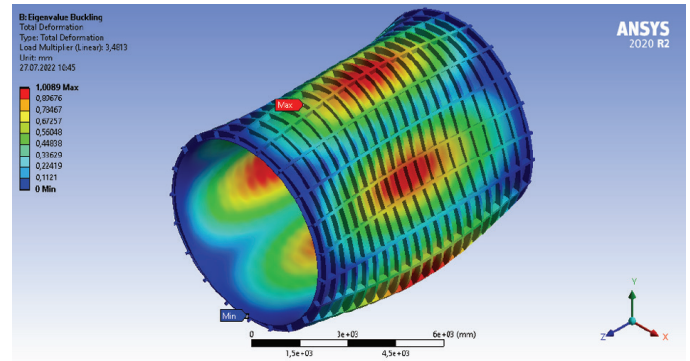


Figure 16. T-sections stiffened combined externally system isometric view.

Table 9. T-reinforced stiffened systems with the same critical buckling pressure produced as a result of optimisation.

Geometry	Transverse internal reinforced system	Longitudinal internal 21 reinforcements system	Transverse external reinforced system	Combined internally reinforced system	Combined external reinforced system
Support element	T Profile	T Profile	T Profile	T Profile	T Profile
Flange thickness (mm)	41.5	32.4	41.9	39.9	39.8
Web thickness (mm)	16.5	12.1	14.8	10.1	14.0
Shell thickness (mm)	25	120.2	28.7	28.0	27.5
Buckling load factor	3.512	3.502	3.502	3.502	3.503
Critical buckling pressure (MPa)	25.517	25.45	25.449	25.447	25.448
Mass (kg)	58956.89	182086.65	66209.12	67942.18	73565.41
Internal volume (m ³)	244.90	246.44	287.06	245.17	287.06
Distance between frames (mm)	453	934.4	453	453	453

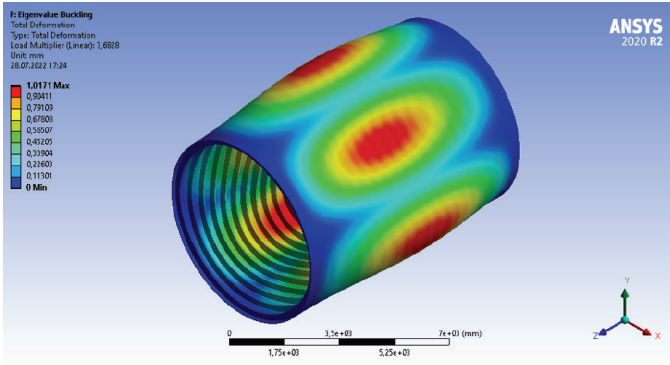


Figure 17. Flat bars stiffened internally system isometric view.

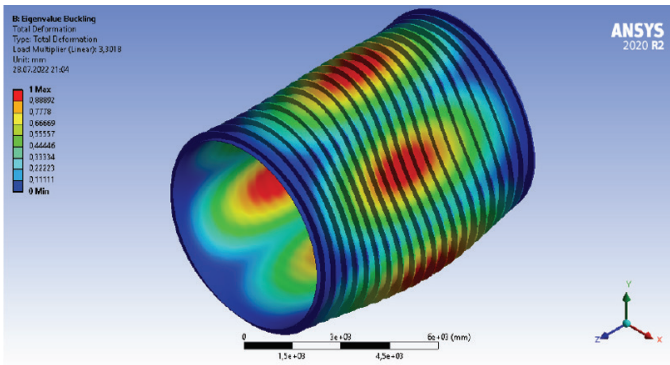


Figure 18. Flat bars stiffened externally system isometric view.

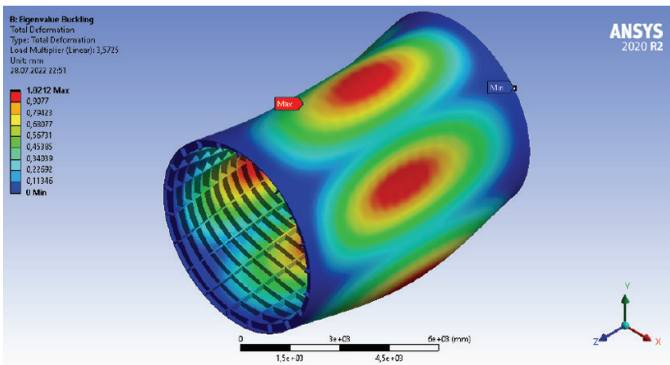


Figure 19. Flat bars stiffened combined system isometric view.

6. Conclusions

Different geometries were investigated for the optimum design of the submarine pressure hull. The objective functions were the lightest structure and the highest internal volume corresponding to the maximum critical buckling pressure. The thicknesses of the structural elements of the pressure hull were the input parameters and the sensitivity of the output parameters on weight and critical buckling pressure were investigated. Different frame profiles were used to investigate the effect of frame geometry on the design. In addition, transverse, longitudinal and combined systems using different frame profiles were investigated and appropriate frames layout was examined. As a result of the optimizations, the minimum weights of the systems with the same critical buckling pressure are given in Table 9. Table 10 shows the flat bar stiffened systems with the same critical buckling pressure. When the results were compared, it is seen that T-sections stiffened systems are more suitable in terms of buckling. When examined in terms of critical buckling pressures at the same weight, transverse internally reinforced system > transverse externally reinforced system > combined internally reinforced system > combined externally reinforced system > longitudinal internally reinforced system.

As can be seen from Table 9, the most ideal design concept in terms of buckling strength is the transverse internal T-sections stiffened system, which is widely used in the construction of many submarine pressure hulls. This system provides the same critical buckling pressure with a lighter weight compared to other systems. Although the Transverse External Reinforced System was advantageous in terms of internal volume, it was disadvantageous compared to the Transverse Internal Reinforced System in terms of weight. The results also indicated that longitudinal reinforcements were insufficient for supporting the submarine pressure hull in terms of buckling strength.

Table 10. Optimization results obtained for flat bar reinforced systems with the same critical buckling pressure.

Geometry	Transverse internal reinforced system	Transverse external reinforced system	Combined internally reinforced system
Support element	Flat bar	Flat bar	Flat bar
Web height (mm)	230	230	230
Web thickness (mm)	49.4	44.2	40.1
Shell thickness (mm)	29.7	34.9	34.3
Buckling load factor	3.502	3.502	3.503
Critical buckling pressure (MPa)	25.443	25.443	25.448
Mass (kg)	78092.40	85201.65	92421.68
Internal volume (m ³)	246.34	287.07	246.34
Distance between frames (mm)	453	453	453

Acknowledgement

This article is extracted from the Master of Science (M.Sc.) thesis, which is entitled “Optimum Structural Design of a Submarine Pressure Hull under Hydrostatic Pressure with Finite Element Method” at the İstanbul Technical University, Institute of Science and Technology, 2022.

Footnotes

Authorship Contributions

Concept: B. Eyiler, and E. Bayraktarkatal., Design: B. Eyiler, and E. Bayraktarkatal., Data Collection or Processing: B. Eyiler, and E. Bayraktarkatal., Analysis or Interpretation: B. Eyiler, and E. Bayraktarkatal., Literature Search: B. Eyiler, and E. Bayraktarkatal., Writing: B. Eyiler, and E. Bayraktarkatal.

Conflict of Interest: No conflict of interest was declared by the authors.

Financial Disclosure: The authors declared that this study received no financial support.

7. References

- [1] BBC News Türkçe, “Titanik’i ziyaret ederken iletişimi kesilen denizaltı hakkında neler biliyoruz?” Accessed: Nov 28, 2024. [Online]. Available: <https://www.bbc.com/turkce/articles/cw0xx17r9d2o>
- [2] S. Chakraborty, “Introduction to submarine design,” Marine Insight, 2019. [Online]. Available: <https://www.marineinsight.com/naval-architecture/introduction-to-submarine-design/>.
- [3] J.R. MacKay, and F.V. Keulen, “Partial safety factor approach to the design of submarine pressure hulls using nonlinear finite element analysis,” *Finite Elements in Analysis and Design*, vol. 65, pp. 1-16, 2013.
- [4] R. V. Mises, “The critical external pressure of cylindrical tubes under uniform radial and axial load,” Report no. 366, The David Taylor Model Basin, Washington, 1933.
- [5] M. E. Lurchick, “Plastic axisymmetric buckling of ring-stiffened cylindrical shells fabricated from strain-hardening materials and subject to external hydrostatic pressure,” Report No. 1393, The David Taylor Model Basin, Washington, 1961.
- [6] T. E. Reynolds, “Inelastic lobar buckling of cylindrical shells under external hydrostatic pressure,” Report No. 1392, The David Taylor Model Basin, Washington, 1964.
- [7] A. R. Bryant, “Hydrostatic pressure buckling of a ring stiffened tube,” Report No. NCRE/306, The David Taylor Model Basin, Washington, 1954.
- [8] K. Aileni, P. Prasanna and P. C. Jain, “Buckling analysis of ring stiffened circular cylinders using Ansys,” *Int J Res Appl Sci Eng Technol*, vol. 5, pp. 2287-2296, 2017.
- [9] D. Oh, and B. Koo, “Empirical initial scantling equations on optimal structural design of submarine pressure hull,” *Journal of Advanced Research in Ocean Engineering*, vol. 4, pp. 7-15, 2018.
- [10] H. Kine, “Collapse design optimisation of ring-stiffened cylindrical pressure hulls,” Master’s thesis, University of Stavanger, Stavanger, 2020.
- [11] R. Wei, K. Shen and G. Pan, “Optimal design of trapezoid stiffeners of composite cylindrical shells subjected to hydrostatic pressure,” *Thin-Walled Structures*, vol. 166, pp.108002.
- [12] N. Rathinam, B. Prabu and N. Anbazhaghan, “Buckling analysis of ring stiffened thin cylindrical shell under external pressure,” *Journal of Ocean Engineering and Science*, vol 6, pp. 360-366.
- [13] S. Şenol, “A structural design approach for submarine resistant hull and structural optimization based on finite element method,” Master’s thesis, ITU Institute of Science and Technology, Naval Architecture and Marine Engineering Department, İstanbul, Türkiye, 2021.
- [14] X. Fu, Z. Mei, S. Wang, X. Bai, E. Zhang, G. Chen and H. Li, “Design method of combined stiffened pressure hulls with variable-curvature characteristic,” *Ocean Engineering*, 281. pp. 114685, 2023.
- [15] T. K. L. Shinoka and T. A. Netto, “Structural optimization applied to submarine pressure hulls,” Elsevier, 2024.
- [16] E. Fathallah and M. Helal, “Optimum structural design of deep submarine pressure hull to achieve minimum weight,” *The International Conference on Civil and Architecture Engineering*, vol. 11, pp. 1-22, 2016.
- [17] R. Burcher and L. Rydill, “Concepts in submarine design,” Cambridge Ocean Technology Series, 1995.
- [18] S. Chakraborty, “Understanding structure design of a submarine,” Marine Insight, 2021. [Online]. Available: <https://www.marineinsight.com/naval-architecture/submarine-design-structure-of-a-submarine/>.
- [19] DNV-GL Rules for Classification: Naval Vessels, Part 4 Sub-surface Ships, Chapter 1 Submarines, 2018.
- [20] Bureau Veritas, Rules for the Classification of Naval Submarines, vol. 33, Fransa. 2016.
- [21] A. Alogla, “Numerical study and finite element analysis of submerged cylindrical pressure hull,” *International Journal of Scientific Research in Science, Engineering and Technology*, pp. 381-388, 2020.
- [22] Seyir Defteri, “Denizaltı inşa çeliği-1: HY80, HY100, HY130.” Accessed Nov 28, 2024. [Online]. Available:
- [23] Türk Loydu, Askeri Gemilere Ait Kurallar, vol E, Sec. 111 - Denizaltılar, İstanbul, 2007.
- [24] J. G. Pulos, “Structural analysis and design considerations for cylindrical pressure hulls,” Report No. 1639, The David Taylor Model Basin, 1963.
- [25] P. Foryś, “Optimization of cylindrical shells stiffened by rings under external pressure including their post-buckling behaviour,” *Thin-Walled Structures*, vol. 95, pp. 231-243, 2015.
- [26] ANSYS, Mechanical User’s Guide 2021-R2, vol. 15317, Canonsburg, 2021.